Analytical and Numerical Flash-Algorithms for Track Fits

M. Dima

Dept. of Physics, Campus Box 390
University of Colorado,
Boulder, CO-80309

Flash-algorithm track-reconstruction routines with speed factors 3000-4000 in excess those of traditional iterative routines are presented. The methods were successfully tested in the alignment of the Test Beam setup for the ATLAS Pixel Detector MCM-D modules, yielding a 60 fold increase in alignment resolution over iterative routines, for the same amount of alocated CPU time.

I. INTRODUCTION

In many particle physics experiments high-precision alignment can be performed provided there is sufficient data and enough computer (CPU) time alocated. While statistics may suffice for many experiments, CPU time can only be decreased through the use of flash reconstruction routines. For instance in pixel detectors, alignment parameters can be tuned iteratively to satisfy good track reconstruction in all events. However, reconstruction of all tracks in all events, for each iteration in alignment parameter space[1], is CPU exhausting and in practice can only be applied to blocks of tracks. If the track fits themselves are also iterative [2], double-nesting of iteration loops occurs and CPU times reach on the order of months. On the other hand if track fits are semi/analytical, CPU times drop 3-4 orders in magnitude and such an approach becomes feasable.

The paper starts with the basic χ^2 fit, examines the validity of the standard quadratic approximation for χ^2 and presents analytical and semi-analytical track reconstruction algorithms, together with CPU-clocked examples[2]. The methods were developed gradually from the simple case of straight tracks (magnetic field free environment, or high momentum tracks), to the more demanding case of helical tracks. The Test Beam setup of the ATLAS Pixel Detector [3] MCM-D modules [4] was used as prototype example for the applied methods, although the latter methods are general and applicable to a number of detectors using tracks.

---

[1]An example of an analytical alignment procedure (*vs.* an iterative one) is illustrated in [1] for the SLD End-Cap Čerenkov Ring Imaging Detector.

[2]The tests were performed on a DEC-ALPHA 878 machine, with EV 5.6 processor at 433 MHz, 640 MB RAM, and running under OSF1 V4.0. Coding was performed in FORTRAN.

II. GENERAL FITS

The general expression for χ^2 in a fit is the sum of the squared normalised residuals over the set of experimental points:

$$\chi^2 \overset{\text{def}}{=} \sum_{j=1}^{N} \left(\frac{\vec{\Delta}_j}{\sigma_{j(\Delta)}} \right)^2 \tag{1}$$

where the error of the jth-residual $\sigma_{j(\Delta)}$ is related to the direction of the residual itself, $\vec{\Delta}_j$ through the covariance matrix σ_j^2 :

$$\sigma_{j(\Delta)}^2 = \frac{\vec{\Delta}_j \cdot \sigma_j^2 \, \vec{\Delta}_j}{\left(\vec{\Delta}_j \right)^2} \tag{2}$$

leading to:

$$\chi_{exact}^2 = \sum_{j=1}^{N} \frac{\left(\vec{\Delta}_j \right)^2}{\vec{\Delta}_j \cdot \sigma_j^2 \, \vec{\Delta}_j} \tag{3}$$

More often however, a quadratic[3] approximation of χ_{exact}^2 is used:

$$\chi_{approx}^2 \overset{\text{def}}{=} \sum_{j=1}^{N} \vec{\Delta}_j \cdot \sigma_j^{-2} \, \vec{\Delta}_j \tag{4}$$

with the equivalent residual error:

$$\sigma_{j(\Delta)}^2 = \frac{\left(\vec{\Delta}_j \right)^2}{\vec{\Delta}_j \cdot \sigma_j^{-2} \, \vec{\Delta}_j} \tag{5}$$

If a track impacts a point's error ellipsoid at $n = tg(\theta_{incid})$ with respect to one of the principal axes, then approximating $|\Delta_j\rangle$ as perpendicular to the trajectory, the two σ's can be written as:

$$\sigma_{exact}^2 \simeq \frac{\sigma_{xy}^2 + n^2 \sigma_z^2}{1 + n^2}$$
$$\sigma_{approx}^2 \simeq \frac{1 + n^2}{\sigma_{xy}^{-2} + n^2 \sigma_z^{-2}} \tag{6}$$

---

[3] $\vec{\Delta}_j \cdot \sigma_j^{-2} \, \vec{\Delta}_j = \Delta_x^2/\sigma_x^2 + \Delta_y^2/\sigma_y^2 + \Delta_z^2/\sigma_z^2$, for σ_j^2 assumed diagonal.

both reducing to σ_{xy}^2 or σ_z^2 for tracks impacting along one of the principal axes.

The Test Beam stand for the ATLAS Pixel MCM-D modules is a Telescope setup, with 4 tracking elements (Sirocco strip Detectors) and two slots for Pixel Module evaluation. The setup was mounted on a marble optical-bench, itself placed on a rail that allowed it to be moved into the active area of a 1.4 Tesla Spectrometer Magnet. The latter was used to determine the magnetic field influence (x-shifts) in an environment comparable to the ATLAS Detector. The Sirocco strips were mounted along $\Delta z = 1.4$ m of beam-line with a tolerance of ± 0.5 mm. The strips, $30 \mu m$ wide, provided a resolution of $4 \mu m$ in the x- and y-directions, while the Pixels, $50 \mu m \times 400 \mu m$, a resolution on the order of $14 \mu m \times 180 \mu m$ depending on the cast technology [4] of the chips. The error matrices of the Test Beam stand Telescope points had thus associated ellipsoids with aspect ratios of 1:125, the difference between fitting a 3D-line to these σ's and one to spherical σ's being 0.1 μm in the Telescope's mid-plane.

The difference between χ_{exact}^2 and χ_{approx}^2 depends strongly on the impact angle of the track onto the individual error ellipsoids:

$$\frac{\Delta \chi^2}{\chi_{exact}^2} = \frac{\left(\sigma_{xy}/\sigma_z\right)^2 + \left(\sigma_z/\sigma_{xy}\right)^2 - 2}{\left(n + 1/n\right)^2} \qquad (7)$$

For the Telescope setup the track's impact angle was on the average 0.15 mrad, with a corresponding $\Delta \chi^2/\chi_{exact}^2$ on the order of 0.02%. When the tracks impact however at an arbitrary angle, $\Delta \chi^2/\chi_{exact}^2$ can reach as high as 3000 for the current σ_z/σ_{xy} ratio, even if $\Delta \sigma^2/\sigma_{exact}^2$ is on the order of unity.

For tracks impacting all points at a constant angle ("stiff"-tracks), $\Delta \chi^2$ is constant along the trajectory and the two methods yield identical results. If the track is measured however piecewise in two different sub-systems, or it is composed of an ensemble of points with different σ's (different types of detectors), then even for straight tracks the two solutions differ. For tracks bending in magnetic field, the track's impact angle changes continuously along the track, $\Delta \chi^2$ following as:

$$d\left(\frac{\Delta \chi^2}{\chi_{exact}^2}\right) \Big/ \frac{\Delta \chi^2}{\chi_{exact}^2} = \frac{dn}{n} \cdot 2 \frac{1 - n^2}{1 + n^2} \qquad (8)$$

Within the 1.4 m of the Telescope, the 180 GeV/c tracks used bend in the B = 1.4 T magnetic field equivalently to $\Delta \chi^2/\chi_{exact}^2 \simeq 0.02\%$ up front and 16% downstream, the approximative method pulling the fit increasingly tighter towards the end - on the order of 0.5 μm per point. The effect is evidently insignificant, both in the Telescope setup, as well as in the real B-physics context of AT-LAS, meaning 2 Tesla magnetic field, tracks of momentum greater than 1 GeV/c, and a measured track length of approximately 0.14 m. Over this span the expected point to point change in χ^2 is less than 4 % per %-$\Delta \chi^2$.

III. LINE FITS

In most cases it is possible to interchange the non-linear expression (3) with its quadratic approximation (4), allowing analytical solutions to be given for "stiff-tracks" i.e. - particle out of magnetic field, weak field with respect to track momentum, or distance travelled small with respect to existing resolution.

The simplest fit is for $\sigma_j^2 = \sigma^2 \cdot \mathbf{1} = const.$:

$$\chi^2 = \sum_{j=1}^{N} \left(\vec{\Delta}_j \right)^2 = min. \qquad (9)$$

Parametrising the tracks as:

$$\vec{r} = \vec{r}_0 + \lambda \vec{n} \qquad (10)$$

with $\vec{n}^2 = 1$ and $\vec{r}_0 \cdot \vec{n} = 0$, equation (9) becomes:

$$\chi^2 = \sum_{j=1}^{N} \vec{\delta}_j^2 = min. \qquad (11)$$

where $\vec{\delta}_j = \vec{r}_j - \vec{r}_0 - \lambda_j \vec{n}$. The minimum condition implies locally $\lambda_j = \vec{r}_j \cdot \vec{n}$ and globally:

$$\vec{r}_0 = (\mathbf{1} - \vec{n}\vec{n}) \langle \vec{r} \rangle$$
$$\mathbf{M} \, \vec{n} = \mu_0 \, \vec{n} \qquad (12)$$

where $\langle \vec{r} \rangle$ denotes average over measured points, and $\mathbf{M} = \langle \vec{r}\vec{r} \rangle - \langle \vec{r} \rangle \langle \vec{r} \rangle$ the spread ellipsoid of points around $\langle \vec{r} \rangle$. The 3 eigen-values of $\mathbf{M}$ represent the length of the track (μ_0), and the two transversal variances to the line-fit.

For $\sigma_j^2 = diag(\sigma_x^2, \sigma_y^2, \sigma_z^2) = const.$ equation (11) holds again, however in normalised form, with $\vec{r}_i \to \sigma^{-1}\vec{r}_i$, $\vec{r}_0 \to \sigma^{-1}\vec{r}_0$ and $\vec{n} \to \sigma^{-1}\vec{n}$. Adapted to the geometry of the Telescope this solution has been clocked to 0.033 μs/2D-fit and 2.6 μs/3D-fit. These times are half or less for current 1000-1500 MHz clock machines. CPU-wise this allows the alignment to be performed using blocks of tracks. The intuitive picture of this procedure is aligning two incomplete 3D images: where there is a track, there is a pixel on the image. The more tracks in an alignment loop, the more pixels per image, and the better the alignment. This idealistic picture is cut cold however, by either lack of data, or of CPU power. In most of the contemporary HEP experiments the limiting factor is CPU power, as the reconstruction of the objects used in the alignment (in this case tracks) can be quite CPU costly. Eliminating this problem with flash-algorithms opens the way to high accuracy alignment. The increase in alignment resolution is proportional to $\sqrt{N_{block}}$, and the CPU cost to N_{block}. Holding CPU time fixed, any speed increase can be equivalenced to a resolution increase. Thus a factor of 4000 in speed, would be equivalent to a factor of 63 in resolution. To exemplify this, consider the

Test Beam setup, where the tracks impact the Sirocco planes at almost normal incidence. At precisely normal incidence any z-misalignment would be un-noticed. The tracks do impact however at an angle on the order of 0.15 mrad, giving an alignment "lever arm" for Δz misalignments on the order of 0.15 μm/mm. With the existing Sirocco resolution ($\simeq 4$ μm) the resolving power (per track) for Δz would be on the order of 27 mm. Increasing the number of tracks per one Δz misalignment loop the resolution improves dramatically, as illustrated in figure 1.
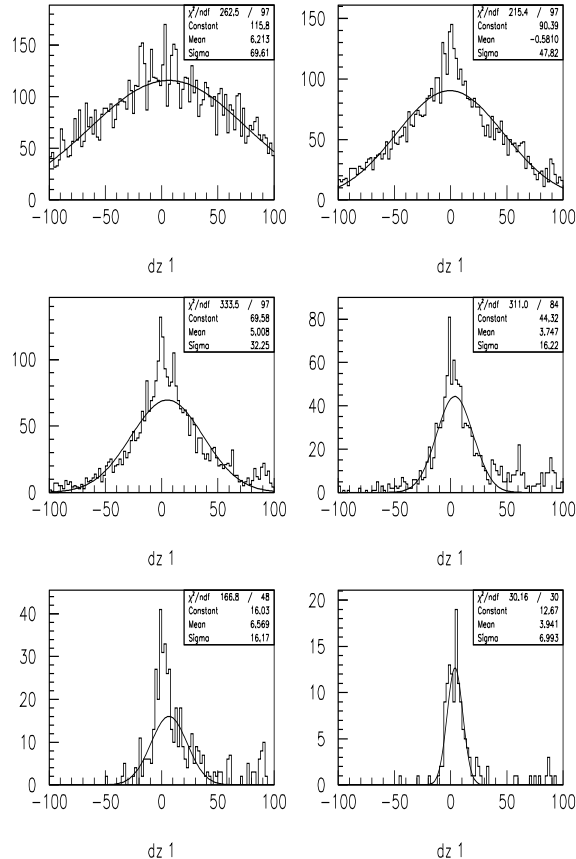

FIG. 1. Translational alignment parameter (Δz) histograms for blocks of 2, 4, 8, 20, 40 and 80 tracks, for Sirocco Plane 1. The effective number of track-fits in each histogram is $\simeq 3$ million. Although in the Telescope setup the alignment lever arm for Δz is very low (0.15 μm/mm, with a $\sigma = 4$ μm detector resolution), the plots show a dramatic improvement in Δz resolution with increasing number of tracks (N_{block}) per iterative alignment loop. The electronics noise is cut-down by a factor of $1/\sqrt{N_{block}}$. The approach demands however extensive CPU power, analytical solutions being needed in order to keep the problem within the capabilities of existing resources. All figures are in mm.

Any multi-tile pixel detector benefiting from this high precision alignment method would better perform in physics involving the resolution of vertices. With the increasing energy frontier (LHC, TESLA/NLC) particle ID techniques are replaced with other means of signal identification. Signal "concentrators" that can serve this purpose are the B-mesons. Their identification depends crucially on vertexing resolution[4].

An improvement to the example considered would be to include in the track fit also the Pixel Demonstrator points. This would mean fitting to points with different error ellipsoids and the imposibility of "absorbing" all σ's into $\vec{r}_0$ and $\vec{n}$ in an unique way, as done previously. For such $\sigma_i^2 \neq \sigma_j^2$ cases, the solution is given by a set of self-consistent equations:

$$\lambda_j = \frac{\vec{n} \cdot \sigma_j^{-2}(\vec{r}_j - \vec{r}_0)}{\vec{n} \cdot \sigma_j^{-2}\vec{n}}$$

$$\vec{r}_0 = \langle \vec{r} \rangle - \langle \lambda \rangle \vec{n}$$

$$\vec{n} = \frac{\langle \lambda \vec{r} \rangle - \langle \lambda \rangle \langle \vec{r} \rangle}{\langle \lambda^2 \rangle - \langle \lambda \rangle^2} \tag{13}$$

solvable semi-analytically in approximately 3 iterations, starting from the previous analytically exact solution.

The approach used in this paper was to tune the alignment[5] by looping over the reconstruction of 2000 tracks, the alignment residuals of the Telescope Sirocco plane-1 being shown in figure 2 (top). The Pixel Detectors under evaluation were to first order aligned analytically (exact solution), and subsequently tuned in a fashion similar to that of the Sirocco planes, in order to compensate for the effect of the low y-resolution on the better x-resolution. The difference between the Pixel demonstrator measured and Telescope predicted positions of the track hits is shown in figure 2 (middle and bottom) for a set of two Pixel Detectors under test. The identical *side*-resolution of the pixels in the x and y-directions (fit

---

[4]For example selecting B-events with high purities and efficiency can be achieved by applying a minimally missing $\vec{p}_\perp$ correction to the m_π evaluated vertex mass [5,6]. In the AT-LAS context $\vec{p}_\perp$ would most likely be referenced to the axis of the jet containing the B sub-jet. The method depends crucially on the vertexing accuracy, yielding for instance at SLD [6] B-events with sample purities on the order of 91-99 % and 65-20% corresponding efficiencies.

[5]The alignment consisted of two separate stages, firstly out of magnetic field, and secondly in magnetic field. In both cases the translational and rotational degrees of freedom were firstly determined for the 4 Sirocco planes. The Pixel Modules were aligned with respect to the Telescope's Sirocco planes. The alignment in magnetic field required an external marker, which was the setup's trigger: a PIN Diode. Its change in image with magnetic field, on a "focal" plane, determined the absolute shifts in the tracking elements of the Telescope setup (the 4 Sirocco planes), and by reference, those of the Pixel Modules under evaluation.

parameter P3) - expected from uniform technology on the chip - gives credit that the alignment conducted to physically tangible results.
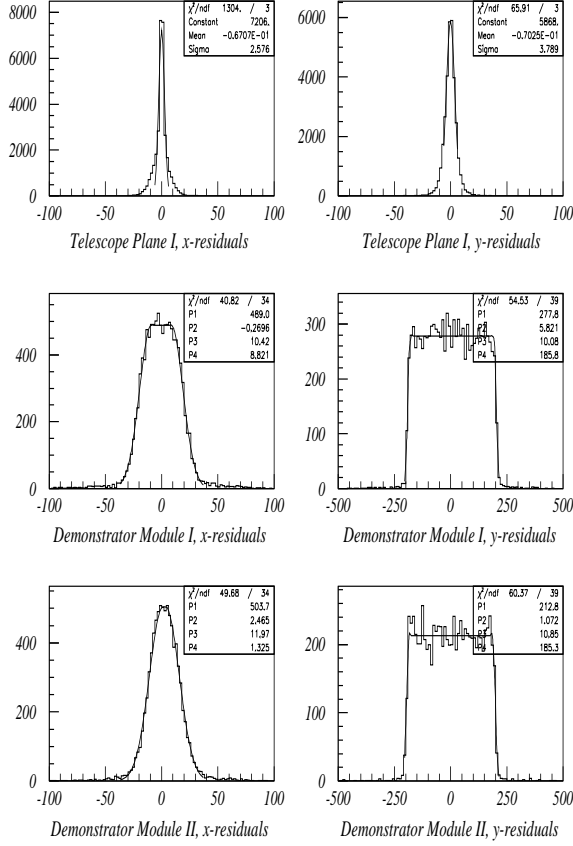

FIG. 2. Final alignment residuals for the Telescope's Sirocco Plane-1 (top), $\sigma_x \simeq 3$ μm, $\sigma_y \simeq 4$ μm, and for two Pixel Detectors under evaluation, cast in different technologies (middle and bottom). The equal *side*-resolution of the Pixels (fit parameter P3, $\sigma_{side} \simeq 11\mu$m, essentially a measure of charge division resolution between pixels) in the x and y-directions gives confidence that the alignment conducts to physically meaningful results. Fit parameter P4 gives the single-hit resolution of the pixel "hat" ($\sigma_{hat} = 1 \ldots 10\mu$m, basically the pixel's geometrical resolution minus the *side*-resolution). The center "thinning" of the Sirocco x-residuals (from a gaussian) by $\simeq 1$ μm was due to the residual magnetic field of the Spectrometer Magnet, as Lorentz drift of the charge carriers in the strips. All figures are in μm.

IV. HELIX FITS

Track fits over small arcs of helices are very sensitive to the fluctuations of the experimental points. The radius of curvature (giving the momentum, or conversely the magnetic field) has consequently a large error, due to the points moving within their error bars. To reduce the errors of such "weak" parameters, fits to collections of tracks - experiencing the same conditions (magnetic field in this case) are used. Iterative fit routines consum however between 90000-300000 μs/3D helix-fit, the previously illustrated method (figure 1) being inapplicable in this case. On the other hand, although desired, flash semi-analytical algorithms for helix-fits are non-trivial to derive. Most of contemporary High Energy Physics experiments however involve large energies and the helical tracks span typically less than 1° of an arc (0.2^o in the case of the Telescope). It is possible then in such cases to perform 3D-helix fits semi-analytically, by perturbatively curving a line-fit into a helix-fit.

The helix equations are:

$$d_t \, \vec{p} = \frac{ec^2}{E} \, \vec{p} \times \vec{B}$$

$$d_t \, \vec{r} = c^2 \, \vec{p}/E \qquad (14)$$

where E is the particle's energy, $\vec{p}$ its momentum and $\vec{B}$ the magnetic field. The solution to equations (14) is:

$$\vec{r} = \vec{r}_0 + \lambda\vec{n} + \frac{\lambda^2}{2!} f\left(\frac{\lambda}{R}\right) \mathbf{F} \, \vec{n} + \frac{\lambda^3}{3!} g\left(\frac{\lambda}{R}\right) \mathbf{G} \, \vec{n} \qquad (15)$$

where $\lambda = \vec{v}_0 t = \omega R t$ is a "linear" distance travelled by the particle, $\vec{\omega} = |e|c^2\vec{B}/E$ the helical rotation pulsation, $\vec{n} = \vec{p}_0/p_0$ the direction of engagement of the particle onto the magnetic field, $\vec{n}_B = e\vec{B}/|e|B$, $R = p_0/|e|B$ a parameter related to the radius of curvature of the helix $R_{helix} = R\sqrt{1 - (\vec{n} \cdot \vec{n}_B)^2}$, $f(\zeta)$ and $g(\zeta)$ two functions:

$$f(\zeta) = \frac{2!}{\zeta^2}(1 - cos\zeta) \; \overset{\zeta \to 0}{\simeq} \; 1$$

$$g(\zeta) = \frac{3!}{\zeta^3}(\zeta - sin\zeta) \; \overset{\zeta \to 0}{\simeq} \; 1 \qquad (16)$$

respectively $\mathbf{F}$ and $\mathbf{G}$ two tensors:

$$\mathbf{F} = \times \vec{C}$$
$$\mathbf{G} = \vec{C}\,\vec{C} - \vec{C}^2 \cdot \mathbf{1} \qquad (17)$$

that satisfy $\mathbf{F}^\dagger = -\mathbf{F}$, $\mathbf{G}^\dagger = \mathbf{G}$, $\mathbf{F}\,\mathbf{G} = \mathbf{G}\,\mathbf{F} = -\vec{C}^2\mathbf{F}$, $\mathbf{F}^2 = \mathbf{G}$, and $\mathbf{G}^2 = -\vec{C}^2\mathbf{G}$. The vector $\vec{C}$ is $\vec{n}_B/R$.

It is evident that for $R \to \infty$ (or equivalently $\lambda \to 0$), expression (15) reduces to the parametrisation of the line (10) used in performing line fits - which is the requirement for the perturbative approach. In most experiments the third order approximation $f(\zeta) \simeq 1$ and $g(\zeta) \simeq 1$ holds up to the following limiting factors:

- **geometric** - the arc of helix should not exceed a length beyond the approximation validity for $f(\zeta)$ and $g(\zeta)$. This is related to the demanded resolution σ and the particle's momentum:

$$p \geq \frac{\lambda}{16(\sigma/\lambda)^{1/3}} \simeq 5 \text{ GeV/c} \qquad (18)$$

4

where in the above, λ and σ are expressed in [m] and p in [GeV/c]. The value for the momentum is for the Telescope setup.

- **dE/dx** - the loss of energy along the trajectory determines a "tighter" helix, the deviation:

$$\sigma = \frac{\lambda^2 E}{2\pi p^2 c^2}\left(\frac{dE}{dx}\right) \tag{19}$$

  needing to be smaller than 4 times the allowed tolerance in the Pixel plane.

- **multiple scattering** - multiple deviations from the direction of flight add up to a displacement of:

$$\sigma \simeq 0.6\lambda\theta_{rms} \tag{20}$$

  where λ is expressed in [mm], θ_{rms} [7] in [mrad] and σ in [μm]. This should determine an error in the Pixel plane no larger than the allowed tolerance.

The semi-analytical helix fit procedure has 3 steps:

1. Estimation of $\vec{n}$, the engagement direction of the particle onto the magnetic field. This is obtained with small CPU demand via a 3D line flash-fit to the first 3-4 points of the trajectory. The vector $\vec{n}$ is an eigen-vector of $\mathbf{M} = \langle\vec{r}\vec{r}\rangle - \langle\vec{r}\rangle\langle\vec{r}\rangle$, hence any perturbation $\delta\mathbf{M} = \mathbf{M}_{helix} - \mathbf{M}_{line}$ changes it only to second order, and for numerical purposes $\vec{n}$ can be considered constant.

2. Using the $\vec{n}$ found above, the second order term corrections to $\vec{r}_0$ and λ_i can be estimated:

$$\Delta\lambda_i = \frac{\lambda_i}{R}(\vec{r}_i - \vec{r}_0)\cdot\vec{n}\times\vec{n}_B$$
$$\Delta\vec{r}_0 = \langle\vec{r}\rangle - \vec{r}_0 - \langle\lambda\rangle\vec{n} - \frac{\langle\lambda^2\rangle}{2R}\vec{n}\times\vec{n}_B \tag{21}$$

  computations again only modestly CPU demanding.

3. Introducing the third order term and using the previously corrected $(\vec{n}, \vec{r}_0, \lambda_i)$, local and global equations for the parameters can be written:

$$(\vec{n} + \lambda_i\mathbf{F}\,\vec{n} + \frac{\lambda_i^2}{2}\mathbf{G}\,\vec{n})\cdot\vec{\rho}_i = 0$$
$$\langle(\lambda\cdot\mathbf{1} - \frac{\lambda^2}{2}\mathbf{F} + \frac{\lambda^3}{6}\mathbf{G})\vec{\rho}\,\rangle = 0$$
$$\langle\,\vec{\rho}\,\rangle = 0 \tag{22}$$

  where $\vec{\rho}_i$ are the residuals of the points to the fitted curve:

$$\vec{\rho}_i = -\vec{r}_i + \vec{r}_0 + \lambda_i\vec{n} + \frac{\lambda_i^2}{2}\mathbf{F}\,\vec{n} + \frac{\lambda_i^3}{6}\mathbf{G}\,\vec{n} \tag{23}$$

Expanding to first order, the corresponding corrections $(\Delta\vec{n}, \Delta\vec{r}_0, \Delta\lambda_i)$ must satisfy:

$$\alpha_i\Delta\lambda_i + \vec{a}_i\cdot\Delta\vec{n} + \vec{b}_i\cdot\Delta\vec{r}_0 + \beta_i = 0$$
$$\langle\vec{a}\,\Delta\lambda\rangle + \langle\lambda^2\rangle\mathbf{1}\cdot\Delta\vec{n} + \mathbf{D}\,\Delta\vec{r}_0 + \vec{\delta} = 0$$
$$\langle\vec{b}\,\Delta\lambda\rangle + \mathbf{D}^\dagger\Delta\vec{n} + \mathbf{1}\cdot\Delta\vec{r}_0 + \vec{\sigma} = 0 \tag{24}$$

where:

$$\alpha_i = \vec{n}^2 - \vec{r}_i\cdot\mathbf{F}\,\vec{n} + \vec{r}_0\cdot\mathbf{F}\,\vec{n}$$

$$\beta_i = \vec{r}_0\cdot\vec{n} - \vec{r}_i\cdot\vec{n} + \lambda_i\vec{n}^2 + \lambda_i\vec{r}_0\cdot\mathbf{F}\,\vec{n}-$$
$$\lambda_i\vec{r}_i\cdot\mathbf{F}\,\vec{n} + \frac{1}{2}\lambda_i^2\vec{r}_0\cdot\mathbf{G}\,\vec{n} - \frac{1}{2}\lambda_i^2\vec{r}_i\cdot\mathbf{G}\,\vec{n}+$$
$$\frac{1}{6}\lambda_i^3\vec{n}\cdot\mathbf{G}\,\vec{n}$$

$$\vec{a}_i = \vec{r}_0 - \vec{r}_i + 2\lambda_i\vec{n} + \lambda_i\mathbf{F}\,\vec{r}_i - \lambda_i\mathbf{F}\,\vec{r}_0$$

$$\vec{b}_i = \vec{n} + \lambda_i\mathbf{F}\,\vec{n}$$

$$\vec{\delta} = \langle\lambda\rangle\vec{r}_0 - \langle\lambda\vec{r}\rangle + \langle\lambda^2\rangle\vec{n} + \frac{1}{2}\mathbf{F}\,\langle\lambda^2\vec{r}\rangle-$$
$$\frac{1}{2}\langle\lambda^2\rangle\mathbf{F}\,\vec{r}_0 + \frac{1}{6}\langle\lambda^3\rangle\mathbf{G}\,\vec{r}_0 - \frac{1}{6}\mathbf{G}\,\langle\lambda^3\vec{r}\rangle+$$
$$\frac{1}{12}\langle\lambda^4\rangle\mathbf{G}\,\vec{n}$$

$$\vec{\sigma} = \vec{r}_0 - \langle\vec{r}\rangle + \langle\lambda\rangle\vec{n} + \frac{1}{2}\langle\lambda^2\rangle\mathbf{F}\,\vec{n} + \frac{1}{6}\langle\lambda^3\rangle\mathbf{G}\,\vec{n}$$

$$\mathbf{D} = \langle\lambda\rangle\mathbf{1} - \frac{1}{2}\langle\lambda^2\rangle\mathbf{F} \tag{25}$$

By eliminating $\Delta\lambda_i = -(\beta_i + \vec{a}_i\Delta\vec{n} + \vec{b}_i\Delta\vec{r}_0)/\alpha_i$ equations (24) become:

$$\mathbf{M}\,\Delta\vec{n} + \mathbf{N}\,\Delta\vec{r}_0 = \vec{\tau}$$

$$\mathbf{N}^\dagger\Delta\vec{n} + \mathbf{R}\,\Delta\vec{r}_0 = \vec{\pi} \tag{26}$$

where:

$$\mathbf{M} = \Big\langle\frac{\vec{a}\,\vec{a}}{\alpha}\Big\rangle - \langle\lambda^2\rangle\mathbf{1}$$

$$\mathbf{N} = \Big\langle\frac{\vec{a}\,\vec{b}}{\alpha}\Big\rangle - \langle\lambda\rangle\mathbf{1} + \frac{1}{2}\langle\lambda^2\rangle\mathbf{F}$$

$$\mathbf{R} = \Big\langle\frac{\vec{b}\,\vec{b}}{\alpha}\Big\rangle - \mathbf{1} \tag{27}$$

and :

$$\vec{\tau} = \vec{\delta} - \Big\langle\frac{\beta\,\vec{a}}{\alpha}\Big\rangle$$

$$\vec{\pi} = \vec{\sigma} - \Big\langle\frac{\beta\,\vec{b}}{\alpha}\Big\rangle \tag{28}$$

5

To zero[th] order the three $\mathbf{M}$, $\mathbf{N}$ and $\mathbf{R}$ tensors are proportional to $(\mathbf{1}-\vec{n}\vec{n})$, the non-invertable perpendicular projection to $\vec{n}$, by factors of $\langle\lambda^2\rangle$, $\langle\lambda\rangle$ and 1. Therefore in the numerical approach, the inversion is obtained by decomposing the operators into a part proportional to $(\mathbf{1}-\vec{n}\vec{n})$ and a "remainder":

$$\mathbf{R} = (\mathbf{1} - \vec{n}\vec{n}) \cdot (2tr\mathbf{R} - \mathbf{R}_{\vec{n}\,\vec{n}} - \mathbf{R}^{\dagger}_{\vec{n}\,\vec{n}})/4 + ... \quad (29)$$

The solution $(\Delta\vec{n}, \Delta\vec{r}_0, \Delta\lambda_i)$ is therefore:

$$\Delta\vec{n} = (\mathbf{R}\mathbf{N}^{-1}\mathbf{M} - \mathbf{N}^{\dagger})^{-1}(\mathbf{R}\mathbf{N}^{-1}\vec{\tau} - \vec{\pi})$$

$$\Delta\vec{r}_0 = \mathbf{N}^{-1}(\vec{\tau} - \mathbf{M}\Delta\vec{n})$$

$$\Delta\lambda_i = -\frac{1}{\alpha_i}(\beta_i + \vec{a}_i \cdot \vec{n} + \vec{b}_i \cdot \Delta\vec{r}_0) \quad (30)$$

All quantities in this section were considered normalised - i.e. $\sigma^{-1}\vec{r} \to \vec{r}$, although for notation simplicity they were written as the quantities themselves.

The CPU demand of the above 3 steps is under 15 μs. For better precision however, the last step can be repeated twice, bringing the 3D-helix fit to 22 μs. This is at least 4000 times faster than any iterative version of the fit.

To complete the fit in all generality, dE/dx can be incorporated by perturbatively bending a pure helical track into a dE/dx-helix. This would allow in principle to infer the track's mass, although with large errors in certain energy ranges.

Using the fit over blocks of 2000 tracks the alignment in magnetic field was checked and adjusted. The fit was then used on blocks of 10 tracks for a fine scan of the beam energy delivered by the SPS to the Test Beam setup. This was expressed in normal-impact radius of curvature equivalent[6], and it is shown in figure 3 (bottom-right).

V. CONCLUSIONS

Analytical methods were shown to have a dramatic impact on the speed of line and helix fits, bringing down CPU usage by 3-4 orders of magnitude. The methods developed were successfully tested in the alignment and

---

[6]The normal-impact radius of curvature equivalent is the radius of curvature of the particle's track, should the particle impact the field orthogonaly. It is a measure of the particle-momentum, preferred in the context of multiple tracks, when each track impacts the field at a different angle.

data reconstruction of the Test Beam results for the ATLAS Pixel Detector MCM-D modules, and can be of great impact for high precision alignment and reconstruction in all pixel detectors. Such routines could be used for instance by the ATLAS Inner Detector to specify precision $\vec{p}_\perp$ corrections to the m_π evaluated mass of B-vertices, in order to strongly suppress c-decay backgrounds.
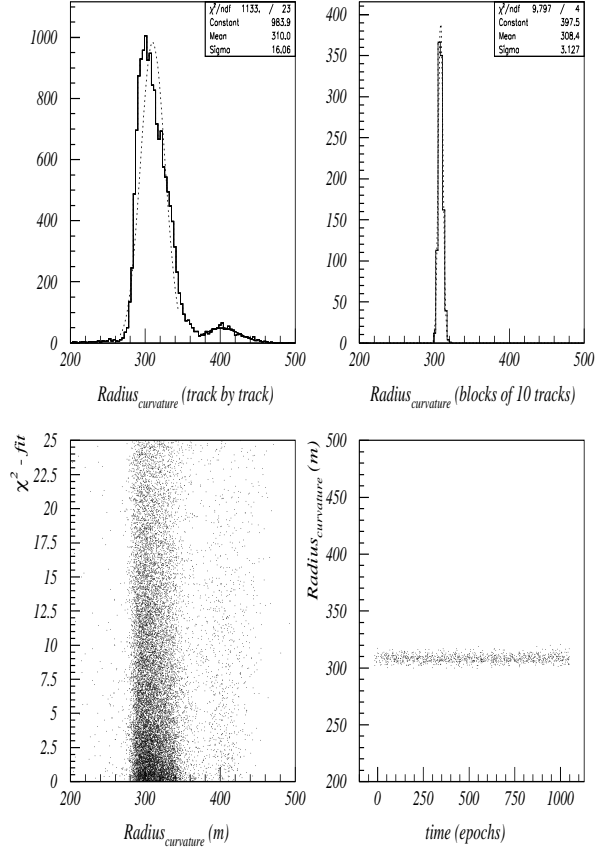

FIG. 3. Normal-impact equivalent radius of curvature for single tracks (top-left) and corresponding χ^2 of fit vs. radius of curvature (bottom-left). The resolution was on the order of 16 m and the average radius of curvature 310 m. Using blocks of 10 tracks (top-right) the resolution improves beyond the statistical factor, to $\simeq$ 3.3 m, the stability of the SPS delivered beam being tracked vs. time bottom-right.

VI. ACKNOWLEDGEMENTS

for support during this period and for the opportunity of better knowing German research and culture.

---

[1] M. Dima, *SLAC-R-0505*, (1997) p. 100.

[2] P. Avery, KWFIT, *CSN98-355*, (1998); Kinematic Fitting Algorithms and Lessons Learned from KWFIT, P. Avery, Feb 2000, in *Padua 2000, Computing in High Energy and Nuclear Physics*, p. 135.

[3] ATLAS Inner Detector TDR, *CERN/LHCC/97-16*, ISBN 92-9083-102-2; *CERN/LHCC/97-17*, ISBN 92-9083-103-0.

[4] I. Ropotar it et al., *Nucl. Instr. Meth.* **A**439 (2000), 536.

[5] ALEPH Collaboration (R. Barate et al.), *Phys.Lett.* **B**401 (1997), 150.

[6] SLD Collaboration (K. Abe et al.), *Phys.Rev.Lett.* 80 (1998), 660.

[7] Particle Data Group, *Euro. Phys. J.* **C**15 (2000), 1.